JURNAL IPTEK
MEDIA KOMUNIKASI TEKNOLOGI
homepage URL : ejurnal.itats.ac.id/index.php/iptek

Torque Characteristic Analysis of Outer Rotor Permanent Magnet Generator for Low Head Hydro Power Application

Pudji Irasari[1], Muhammad Fathul Hikmawan[2] and Puji Widiyanto[3]

[1,2,3]Reserach Center for Electrical Power and Mechatronics, Indonesian Institute of Sciences Bandung, Indonesia

INFORMASI ARTIKEL

Jurnal IPTEK – Volume 23 Nomer 2, Desember 2019

Halaman:
79 – 86
Tanggal Terbit :
31 Desember 2019

DOI:
10.31284/j.iptek.2019.v23i2.524

ABSTRACT

This paper analyzes the torque characteristics of outer rotor PMG for low head hydropower applications. The aim is to prevent the generator torque from exceeding the turbine torque as the prime mover so that the system can work properly in both start and steady-state conditions. The PMG is of outer rotor type and the torques are calculated analytically and numerically. The analysis is focused only on the PMG without connecting it to the turbine. Two analyzed torques include electromagnetic torque and starting torque, which comprises cogging torque, hysteresis torque, and friction torque. The electromagnetic torque was obtained by loading the PMG with resistance and impedance (R_L-L_L in series) respectively. The results indicate that electromagnetic torque is the highest among all the investigated torques although its value is only 5.6% of the turbine torque, and cogging torque is the highest among the starting torque. From those results, it can be concluded that the hydro turbine torque can overcome the generator torque both at the start and steady-state conditions.

Keywords: *PMG; electromagnetic torque; cogging torque; hysteresis torque; friction torque;*

EMAIL

Pudj002@lipi.go.id
muha071@lipi.go.id
puji008@lipi.go.id

PENERBIT

LPPM- Institut Teknologi Adhi Tama Surabaya
Alamat:
Jl. Arief Rachman Hakim No.100,Surabaya 60117,
Telp/Fax: 031-5997244

ABSTRAK

Makalah ini menganalisis karakteristik torsi generator magnet permanen (GMP) rotor luar untuk aplikasi pembangkit listrik tenaga hidro *head* rendah. Tujuannya adalah untuk mencegah agar torsi generator tidak melebihi torsi turbin sebagai penggerak utama sehingga sistem pembangkit dapat bekerja dengan baik dalam kondisi asut maupun kondisi tunak. GMP yang dianalisis adalah dari jenis rotor luar dan torsinya dihitung secara analitik maupun numerik. Dua torsi yang dianalisis meliputi torsi elektromagnetik dan torsi asut yang terdiri dari torsi cogging, torsi hysteresis dan torsi gesekan. Torsi elektromagnetik diperoleh dengan cara membebani GMP masing-masing dengan beban resistansi dan impedansi (resistansi dan induktansi dihubungkan secara seri). Hasil perhitungan dan simulasi menunjukkan bahwa torsi elektromagnetik adalah yang tertinggi di antara semua torsi meskipun nilainya hanya 5.6% dari torsi turbin, dan torsi cogging adalah yang paling besar di antara torsi asut. Dari hasil-hasil tersebut dapat disimpulkan bahwa torsi turbin air dapat mengatasi torsi generator dalam kondisi asut maupun kondisi tunak.

Kata kunci: *GMP; torsi elektromagnetik; torsi cogging; torsi hysteresis; torsi gesekan;*

INTRODUCTION

The utilization of water energy sources for electricity generation has been carried out for decades. To get a lot of energy, the waterfall is widely used by applying high head turbine types,

such as crossflow. However, in recent years, stream with the head less than 5 m is an interesting challenge to be utilized as a power plant, driven by the low price of permanent magnet generators (PMG). Using low-speed PMG on a hydropower plant can reduce or eliminate mechanical transmission so that the power plant becomes more compact. Designing and prototyping of head < 5 m hydropower plants using low-speed PMG were conducted by [1]-[3].

One of the PMG types employed for the low head hydropower plant is outer rotor radial flux. In comparison with the inner rotor type, the outer rotor is better in power density and cooling as the rotor is on the outer side of the generator. Besides, at high speed, centrifugal force strengthens the permanent magnets on the machine frame [4] [5]. Those superiorities make outer rotor PMG is applied not only in power plants [6]-[9] but also in vehicles [10] [11].

LITERATURE REVIEW

In the power generation system, the generator is coupled with a prime mover, which in this case is a low head hydro turbine, to produce electrical power. The flow of power and torque acting on the power system are depicted in Figure 1. Torque is also named the moment of a force. According to Newton's third law, forces of two objects are equal in magnitude and opposite in direction. In compliance with that, in steady-state, the mechanical torque delivered by the turbine should be balanced with the torque produced by the generator. T_{mech1} acting on the shaft is countered by the electromagnetic torque in the air gap T_{elm}. This reaction torque T_{elm} tends to tilt the stator in the direction of rotation. Therefore, T_{mech3} is needed to hold it. On the prime mover housing, T_{mech1} is countered by T_{mech2}. In the system, T_{mech2} and T_{mech3} are in the form of mechanical support (concrete floor). The main shaft connecting the generator and the turbine should be able to bear the highest torque both in normal and fault conditions [12]. Therefore, the shaft must be designed properly so as not to cause twisting or breaking.

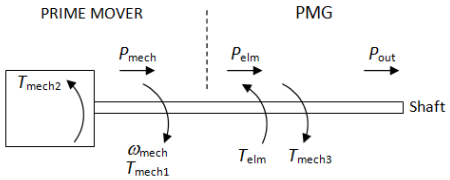

Figure 1. Power flow and torque acting on a power generating system

In this paper, the torque characteristics of 3 kW, 200 rpm, outer rotor PMG under start and steady-state conditions will be discussed. The analysis is focused on the generator by disconnecting it from the turbine. The torques analyzed include starting torque and electromagnetic torque. The starting torque covers cogging torque, hysteresis torque and friction torque [13]. And the electromagnetic torque is observed under loads of resistance and impedance (resistance and inductance in series) respectively. The mechanical torque of the hydro turbine is separately calculated and the result is around 190 N.m.

Starting Torque

During start (no-load condition), the torque of PMG comprises cogging torque T_c, hysteresis torque T_{hys} and the torque due to the friction of bearing and seal T_{fric}, so that starting torque T_{start} can be written as,

$$T_{start} = T_c + T_{hys} + T_{fric} \quad \text{..... (1)}$$

Cogging Torque

Cogging torque is an inherent characteristic of PMG due to the interaction between permanent magnets on the rotor and the teeth of the stator. Permanent magnets generate magnetic flux in the

air gap and salient stator causing the variation of air gap reluctance. This relationship is expressed as,

$$T_c = -\frac{1}{2}\phi_g^2 \frac{d\Re}{d\theta} \quad \text{..... (2)}$$

where ϕ_g is the air gap flux, $\Re$ is the air gap reluctance, and θ is the rotor position [14].

The attraction/repulsion cycles between permanent magnet and stator teeth occur periodically, so T_c can also be stated in Fourier series,

$$T_c = \sum_{k=1}^{\infty} T_{mk} \sin(mk\theta) \quad \text{..... (3)}$$

where m is the least common multiple of the number of stator slots and the number of poles, k is an integer, and T_{mk} is a Fourier coefficient. The periodicity is indicated by m, which is the mechanical evolution of the rotor [15]. On toothless machines, T_c is zero.

Cogging torque is usually larger than the hysteresis and friction torque and a major factor of a high starting torque [13] [16]. To decrease cogging torque, in this paper, fractional winding with the number of slots per pole per phase 1.5 is applied. The magnets are not skewed and the pole arc to pole pitch ratio is 0.8. T_c is numerically calculated using FEMM 4.2 software.

Hysteresis Torque

The second component of starting torque is hysteresis loss. This loss is caused by a form of intermolecular friction when a varying magnetic field is applied to the magnetic material. This loss is directly proportional to the size of the hysteresis loop of a given material. Therefore, materials with low coercivity have narrow hysteresis loops, which result in low hysteresis loss [17] [18].

Hysteresis torque T_{hys}, is expressed by,

$$T_{hys} = \frac{P_{hys}}{\omega} = \frac{P_{hys}}{2\pi f} \quad \text{..... (4)}$$

where hysteresis loss P_{hys} is found by using equation,

$$P_{hys} = C_h \, f \, B_p^{a+bB_p} \quad \text{..... (5)}$$

with C_h = 0.0025, f =50 Hz, B_p = 1.7 T, a and b are constants influenced by the stator and rotor material, which is a silicon steel sheet. Here, a = 1.8317 and b = -0.0035.

Friction Torque

The last component of starting torque in equation (1) is friction torque, which occurs between shaft and bearing. To support the rotor body, two bearings are needed (Figure 2). The calculation of the shaft dimension and the radial force of the bearing, as well as the selection of the bearing type, were conducted with referring to [19]. The results are 60 mm for the shaft diameter made of carbon steel S45 C, and deep groove ball bearing for the bearing type with serial number 6313 RS1 for both bearing A and bearing B. The radial forces of the bearings are 6544.12 N and 1641.59 N, for bearing A and B respectively.

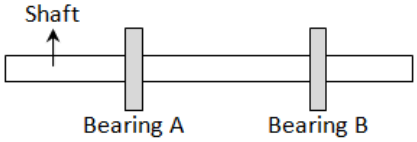

Figure 2. Bearings on the shaft to support the rotor body

During the start, the torque acting on the bearing must be able to overcome the sliding and frictional moment of the seals. The friction torque on bearing A and B is calculated using the following equations,

$$T_{fric} = T_{sl} + T_{seal} \quad \text{..... (6)}$$

$$T_{sl} = G_{sl} + \mu_{sl} \quad \text{..... (7)}$$

$$G_{sl} = S_1 \times {d_m}^{-0.26} \times {F_r}^{5/3} \quad \text{..... (8)}$$

$$T_{seal} = (K_{s1} \times {d_s}^{\beta}) + K_{s2} \quad \text{..... (9)}$$

where: T_{fric} is the start moment of bearing, T_{sl} is the sliding friction moment (N.m), T_{seal} is the friction moment of the seal (N.m), G_{sl} is the sliding friction variables μ_{sl} is the sliding friction coefficient = 0.05, S_1 is the Sliding frictional moment of the bearing = 2.84 x 10^{-3}, d_m is the bearing mean diameter = 102.5 mm, F_r is the radial force of the bearing (N), K_{s1} is the bearing constant that depends on the bearing type = 0.018, K_{s2} is the bearing constant that depends on the bearing and seal types = 20; d_s is the shoulder diameter of the bearing = 88.35, β is the exponent bearing and seal type = 2.25.

Electromagnetic Torque

In a turbine-generator system, the input torque of the PMG is the mechanical torque sent by the turbine shaft. However, considering only the generator, the input torque is the electromagnetic torque. According to the torque flow, the mechanical torque must be larger than the electromagnetic torque to rotate the generator to produce electric power.

Once the rotor of PMG rotates, a rotating magnetic field crosses the air gap and cuts the stator windings or conductors. By Faraday's law, the time-varying flux will induce a voltage in those conductors. The induced voltage is usually also known as electromotive force (EMF), which is denoted by E_f in Table 1.

When the armature windings are connected across the load, the current will flow in each one of them. These current-carrying conductors will, in turn, produce a rotating magnetic field in the air gap with the same speed as the rotating magnetic field from the rotor. This linkage flux develops torque that is called electromagnetic torque or air gap torque and is presented by [20],

$$T_{elm} = \frac{P_{elm}}{\omega} \quad \text{..... (10)}$$

$$P_{elm} = m_1\left[E_f I_{aq} + I_{ad} I_{aq}\left(X_{md} - X_{mq}\right)\right] \quad \text{..... (11)}$$

In this study, the PMG operates off-grid and is loaded with resistance R_L alone and impedance Z_L consists of resistance - inductance (R_L-L_L) in series. The d- and q- axis of the armature current I_a are calculated with [20],

$$I_a = \frac{E_f}{\sqrt{(R_a+R_L)^2+(\omega L_s+\omega L_L)^2}} \quad \text{..... (12)}$$

$$I_{ad} = \frac{E_f(X_{sq}+X_L)}{\sqrt{(X_{sd}+X_L)(X_{sq}+X_L)+(R_a+R_L)^2}} \quad \text{..... (13)}$$

$$I_{aq} = \frac{E_f(R_a+R_L)}{\sqrt{(X_{sd}+X_L)(X_{sq}+X_L)+(R_a+R_L)^2}} \quad \text{..... (14)}$$

METHOD

The studied PMG is connected with the turbine through a mechanical transmission. To obtain a compact construction, the outer diameter of the rotor must not exceed 425 mm. The topology and geometry of the PMG are exhibited in Figure 3.

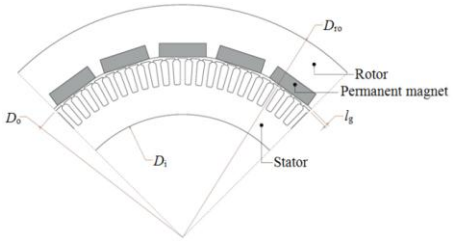

Figure 3. Topology and geometry of the PMG

Furthermore, the dimensions of the stator and rotor, as well as the main electrical parameters at the nominal frequency, are listed in Table 1. As mentioned earlier, the turbine torque has been calculated separately, which has a value of 190 N.m. The methodology of this study is described by the flowchart in Figure 4.

Table 1. The stator and rotor dimensions and the electrical parameters

Descriptions	Value	Unit	Descriptions	Value	Unit
Stator outer diameter[1], D_o	0.300	m	Phase terminal voltage	222	V
Stator inner diameter[1], D_i	0.206	m	Phase induction voltage[2], E_f	238	V
Air gap length[1], l_g	2	mm	Phase armature current[2], I_a	4.54	A
Stator slot numbers	90	slots	Nominal frequency[2], f	50	Hz
Pole numbers	20	poles	Synchronous speed	300	rpm
Phase winding number	450	wdgs	Armature resistance[2], R_a	0.88	Ω
Stator core length	100	mm	Magnetic inductance	6.35	mH
Rotor outer diameter[1], D_{ro}	0.390	m	Synchronous inductance	8.40	mH
PM width	0.038	m	Leakage inductance	2	mH
PM length	0.095	m	d-axis synch. reactance[2], X_{sd}	2.63	Ω
PM height	0.01	m	q-axis synch. reactance[2], X_{sq}	9.43	Ω
Output power	3100	W	d-axis magnetic reactance[2], X_{md}	2	Ω
Phase numbers[2], m_1	3	phases	q-axis magnetic reactance[2], X_{mq}	8.80	Ω

Note: [1] refers to Figure 3, [2] is used in the equation

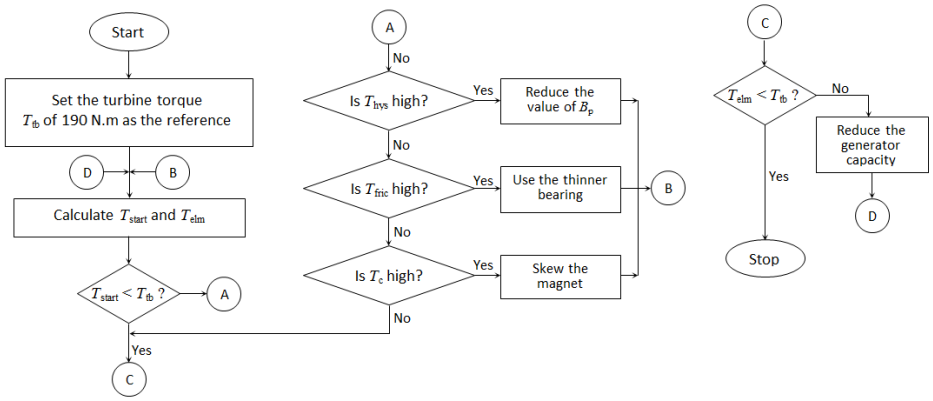

Figure 2. Flowchart for torque characteristics analysis of this study

The definition of "high" for T_{hys}, T_{fric}, and T_c in Figure 4 is decided by the designer with the constraint that $T_{start} < T_{tb}$ should be fulfilled. Reducing T_{hys} can be done by cutting the value of B_p down (Equation (5)). T_{fric} can be lowered by using a thinner bearing, which means having smaller ball bearing size and reducing the friction between the ball surface and both inner and outer rings. Skewing the magnet will decrease the surface area of the magnet facing the stator teeth so that T_c can be reduced. If $T_{start} < T_{tb}$ has been fulfilled, T_{elm} is then analyzed. In Equation (11), T_{elm} is a reciprocal reaction between the magnetic flux of permanent magnet and the flux generated by the current flowing in the conductors. Therefore, reducing T_{elm} can be executed by reducing I_a, which means reducing the capacity of the generator.

RESULT AND DISCUSSION

Cogging Torque and Hysteresis Torque

The simulation of cogging torque is carried out along one slot pitch angle, which is from 0^o to 7^o, and the result is exhibited in Figure 5.

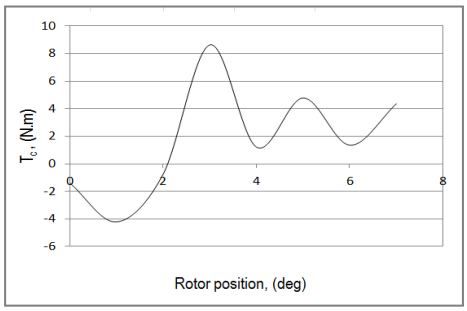

Figure 3. Cogging torque vs. rotor position

The amplitude of the cogging torque wave, from 0° to 3°, indicates the highest peak to peak value, which is 12.86 N.m but it then drops gradually to 3 N.m, from 4° to 7° of the rotor position. According to [13], the value of cogging torque that is taken into account during the starting torque is its peak value. Hence, from Figure 4, T_c is 8.66 N.m, which is still far below the turbine torque or only around 4.56% of the turbine torque. Hysteresis loss P_{hys} and hysteresis torque T_{hys} can be found quickly by using equation (4-5). The results are 15.36 W and 4.89×10^{-2} N.m consecutively. These values are very small and often neglected in some studies.

Friction Torque

The calculation results of T_{sl}, T_{seal}, and T_{fric} on bearing A and B are presented in Table 3. It is already explained above that bearing A and B are of the same type. Therefore, among all the parameters, from equation (6) to (9), it is only F_r that strongly influence T_{fric} on both bearings. Bearing A has a larger F_r due to its position that is closer to the turbine. From Table 2, the total T_{fric} of both bearing A and B is 65.6×10^{-3} N.m.

Table 2. The torques on bearing A and B

No.	Description	Torque (N.m)	
		Bearing A	Bearing B
1	G_{sl}	438.184	69.322
2	T_{sl}	21.91×10^{-3}	3.47×10^{-3}
3	T_{seal}	20.11×10^{-3}	20.11×10^{-3}
4	T_{fric}	42.02×10^{-3}	23.58×10^{-3}

Electromagnetic Torque

In the simulation, R_L and Z_L loads are determined in such a way that the maximum current of the simulation is still around the nominal current of the generator 4.54 A. The calculation results of T_{elm} for each load are presented in Table 3 and 4 respectively and the corresponding graphs of each table are depicted in Figure 6, a and b.

Table 3. Calculation results of T_{elm} under R_L load

No.	R_L (Ω)	I_{ad} (A)	I_{aq} (A)	I_a (A)	P_{elm} (W)	T_{elm} (N.m)
1	50	0.86	4.63	4.67	3388.21	10.79
2	55	0.71	4.22	4.25	3077.49	9.80
3	60	0.60	3.88	3.91	2819.40	8.97
4	65	0.51	3.59	3.61	2601.55	8.28
5	70	0.44	3.34	3.35	2415.15	7.69
6	75	0.39	3.12	3.13	2253.82	7.17
7	80	0.34	2.93	2.94	2112.80	6.73
8	85	0.30	2.76	2.77	1988.47	6.33

Table 4. Calculation results of T_{elm} under R_L & L_L

No.	R_L (Ω)	L_L (H)	Z_L (Ω)	I_{ad} (A)	I_{aq} (A)	I_a (A)	P_{elm} (W)	T_{elm} (N.m)
1	50	0.01	50.10	1.12	4.55	4.69	3352.04	10.67
2	50	0.04	51.55	1.02	4.14	4.27	3043.39	9.69
3	50	0.07	54.62	0.89	3.60	3.71	2635.86	8.39
4	50	0.10	59.05	0.75	3.04	3.13	2218.58	7.06
5	50	0.13	64.56	0.63	2.54	2.61	1842.80	5.87
6	50	0.16	70.90	0.52	2.11	2.17	1526.42	4.86
7	50	0.19	77.86	0.43	1.76	1.81	1268.77	4.04
8	50	0.22	85.30	0.36	1.47	1.52	1061.84	3.38

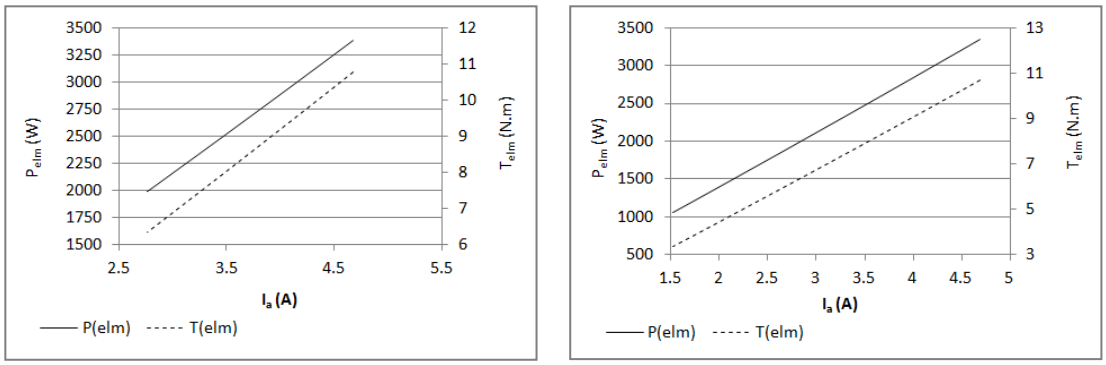

(a) (b)

Figure 6. P_{elm} and T_{elm} characteristics under a load of (a) R_L and (b) Z_L

Under the Z_L load, the R_L is maintained constant so that the effect of the change in L_L can be observed clearly. Under both loads, T_{elm} shows a downward trend, or in other words, T_{elm} is inversely proportional to R_L and L_L loads. The maximum T_{elm} is 10.79 N.m, which is around 5.6% of the turbine torque.

CONCLUSION

The analysis of torque characteristics of outer rotor PMG for low head hydropower applications has been discussed in this paper. The investigated torques include cogging torque, hysteresis torque, friction torque, and electromagnetic torque. The simulation results show that: 8.66 N.m of cogging torque is the largest among the starting torque followed by friction torque and hysteresis torque. Electromagnetic torque is inversely proportional to the load with the highest value of 10.79 N.m that is acquired under 50 Ω of R_L load. In comparison with the turbine torque, the electromagnetic torque is only 5.6%. From all the results, it can be concluded that the generating system can operate well in terms of the turbine's ability to drive the generator.

ACKNOWLEDGMENT

The authors would like to thank the Research Center for Electrical Power and Mechatronics, the Indonesian Institute of Sciences for all the facility support.

REFERENCES

[1] P. Irasari, P. Sutikno, P. Widiyanto, and Q. Maulana, "Performance Measurement of a Compact Generator - Hydro Turbine System," *International Journal of Electrical and Computer Engineering (IJECE)*, vol. 5, pp. 1252-1261 2015.

[2] C. h. Corp., "Very Low Head (VLH) Turbine," in *11th Annual Power of Water Conference*, ed. Ontario, 2011.

[3] R. A. Subekti, A. Susatyo, and P. Irasari, "Design and Analysis of the Prototype of Pico Hydro Scale Submersible Type Turbine-Generator for Flat Flow River Application," *Teknologi Indonesia*, vol. 35, pp. 1-8, 2012.
[4] E. Fornasiero, M. Morandin, E. Carraro, N. Bianchi, and S. Bolognani, "Outer Rotor IPM Generator with Wide Constant Power Region for Automotive Applications," in *ITEC*, Dearborn, MI, USA 15-18 June 2014
[5] I. Tarımer and C. Ocak, "Performance Comparision of Internal and External Rotor Structured Wind Generators Mounted from Same Permanent Magnets on Same Geometry," *Electronics and Electrical Engineering*, vol. 4, pp. 65-70, 2009.
[6] H. A. Lari, A. Kiyoumarsi, B. M. Dehkordi, A. Darijani, and S. M. Madani, "Analysis and Design of a Permanent-Magnet Outer-Rotor Synchronous Generator for a Direct-Drive Vertical-Axis Wind Turbine," *Iranian Journal of Electrical & Electronic Engineering*, vol. 10, 2014.
[7] L. Jian, K. T. Chau, and J. Z. Jiang, "A Magnetic-Geared Outer-Rotor Permanent-Magnet Brushless Machine for Wind Power Generation," *IEEE Transactions on Industry Applications* vol. 45, pp. 954-962, 2009.
[8] J. Chen, C. V. Nayar, and L. Xu, "Design and Finite-Element Analysis of an Outer-Rotor Permanent-Magnet Generator for Directly Coupled Wind Turbines," *IEEE Transactions on Magnetics* vol. 36, pp. 3802-3809, 2000.
[9] Y. Kraimeen, I. Al-Adwan, and M. S. N. Al-Din, "Finite Element Analysis of an Outer Rotor Permanent Magnet Brushless DC Generator," *International Journal of Electrical Engineering*, vol. 6, pp. 99-116, 2013.
[10] W. Fei, P. C. K. Luk, J. Shen, and Y. Wang, "A Novel Outer-Rotor Permanent-Magnet Flux-Switching Machine for Urban Electric Vehicle Propulsion," in *3rd International Conference on Power Electronics Systems and Applications*, Hong Kong, China, 20-22 May 2009.
[11] W. Fei, P. C. K. Luk, J. Shen, Y. Wang, and M. Jin, "A Novel Permanent Magnet Flux Switching Machine with an Outer-Rotor Configuration for In-Wheel Light Traction Applications," *IEEE Transaction on Industry Applications*, vol. 48, pp. 1496-1506, 2012.
[12] J. Machowski, J. W. Bialek, and J. R. Bumby, *Power System Dynamics and Stability*. England: John Wiley & Sons, 1998.
[13] W. Wu, V. S. Ramsden, T. Crawford, and G. Hill, "A Low-Speed, High-Torque, Direct-Drive Permanent Magnet Generator For Wind Turbines," in *IEEE Industrial Application Conference*, 2000, pp. 147-154.
[14] N. Ozturk, A. Dalcalı, E. Celik, and S. Sakar, "Cogging Torque Reduction by Optimal Design of PM Synchronous Generator for Wind Turbines," *International Journal of Hydrogen Energy* vol. 42, pp. 1759 3 - 7600, 2017.
[15] L. Dosiek and P. Pillay, "Cogging Torque Reduction in Permanent Magnet Machines," *IEEE Transactions on Industry Applications* vol. 43, pp. 1565-1571, 2007.
[16] J.-Y. Choi, S.-M. Jang, and B.-M. Song, "Design of a Direct-Coupled Radial-Flux Permanent Magnet Generator for Wind Turbines " in *Power and Energy Society General Meeting, 2010 IEEE* Minneapolis, MN 2010, pp. 1-6.
[17] C. Huynh, L. Zheng, and D. Acharya, "Losses in High-Speed Permanent Magnet Machines Used in Microturbine Applications," *Journal of Engineering for Gas Turbines and Power*, vol. 131, pp. 022301-1 - 022301-6, 2009.
[18] I. Mosincat, "Hysteresis Losses Influence on the Cogging Torque of High-Efficiency Surface Mounted PM Machines," Master Thesis, Department of energy technology, Aalborg University, Denmark, 2011.
[19] P. M. P. Amaro, "Friction Torque in Thrust Ball and Roller Bearings Lubricated with "Wind Turbine Gear Oils" at Constant Temperature," Master Thesis, Mechanical Engineering, University of Porto, Porto, Portugal, 2012.
[20] J. F. Gieras, R.-J. Wang, and M. J. Kamper, *Axial Flux Permanent Magnet Brushless Machines*, 2nd ed.: Springer, 2008.